ANNUAL REVIEWS

Annual Review of Physical Chemistry

Optical Force-Induced Chemistry at Solution Surfaces

Hiroshi Masuhara[1] and Ken-ichi Yuyama[2]

[1]Department of Applied Chemistry and Center for Emergent Functional Matter Science, National Chiao Tung University, Hsinchu 30010, Taiwan; email: masuhara@masuhara.jp

[2]Department of Chemistry, Osaka City University, Osaka 558-8585, Japan; email: yuyama@sci.osaka-cu.ac.jp

Annu. Rev. Phys. Chem. 2021. 72:565–89

First published as a Review in Advance on February 10, 2021

The *Annual Review of Physical Chemistry* is online at physchem.annualreviews.org

https://doi.org/10.1146/annurev-physchem-090419-044828

Keywords

optical trapping, molecular crystallization, nanoparticles, surface, interface, assembly formation

Abstract

When an intense 1,064-nm continuous-wave laser is tightly focused at solution surfaces, it exerts an optical force on molecules, polymers, and nanoparticles (NPs). Initially, molecules and NPs are gathered into a single assembly inside the focus, and the laser is scattered and propagated through the assembly. The expanded laser further traps them at the edge of the assembly, producing a single assembly much larger than the focus along the surface. Amino acids and inorganic ionic compounds undergo crystallization and crystal growth, polystyrene NPs form periodic arrays and disklike structures with concentric circles or hexagonal packing, and Au NPs demonstrate assembling and swarming, in which the NPs fluctuate like a group of bees. These phenomena that depend on laser polarization are called optically evolved assembling at solution surfaces, and their dynamics and mechanisms are elucidated in this review. As a promising application in materials science, the optical trapping assembly of lead halide perovskites, supramolecules, and aggregation-induced emission enhancement–active molecules is demonstrated and future directions for fundamental study are discussed.

1. INTRODUCTION

The laser (light amplification by stimulated emission of radiation) has been contributing to the development of physical chemistry since its invention in 1960 (1). Coherent oscillation from a cavity shows characteristics of light such as monochromaticity, pulse mode, and directionality. This allows light–matter interactions to be studied in more detail and the microscopic nature of molecules to be clarified. The monochromaticity has opened state-to-state chemistry in which a particular rotational, vibrational, and electronic level of the molecule is excited, and the resulting excited state in a specific rotational, vibrational, and electronic energy level undergoes selective relaxation and reaction. This fundamental chemistry on isolated molecules in the gas phase has been one of the major research areas in physical chemistry (2). The pulsed laser was soon introduced to time-resolved spectroscopy, which was originally called flash photolysis before the use of the laser was introduced (3). Nanosecond, picosecond, and then femtosecond chemistry have received a great amount of attention as new frontiers in physical chemistry (4–6). Because the laser can be well focused under a microscope, this allowed the development of many innovative tools and studies, such as optical imaging, super-resolution microscopy, single-molecule fluorescence spectroscopy, and multiplane observation (7–11). In all of this research, laser light is used as an energy source for molecular reactions or as a light source for monitoring physical and chemical processes; in these studies, laser light is generally absorbed, scattered, and/or diffracted. However, light was not widely recognized as a source of mechanical force, and many scientists did not expect chemistry by optical force even when Ashkin and colleagues (12) proposed optical tweezers.

Upon light–matter interaction, the momentum of photons can be transferred to the material, exerting mechanical force on it. This idea was first experimentally tested by Lebedev (13). A large yet lightweight target set in vacuum showed a small tilt when it was irradiated by a conventional light. Now the high-intensity light of lasers can be focused on a small area so that a large transfer of momentum from light to matter is possible. This opens up the new research area of optical manipulation (14–31). Ashkin first demonstrated that a polymer microparticle (MP) can be pushed, levitated, and transferred by two counterpropagating continuous-wave (CW) laser beams in 1970 (32) and proposed optical tweezers by tightly focusing a single laser beam on a single MP (12, 33). This technique was soon applied to biological targets such as living single cells, bacteria, and DNA (34–37). One of the authors of this review (H. Masuhara), with colleagues (38, 39), introduced a Galvano mirror set to microscopic systems and achieved free manipulation of single MPs and single liquid droplets in the focal plane. This idea was then integrated with fluorescence spectroscopy (40), time-resolved absorption spectroscopy (41), microelectrochemistry (42), laser ablation (43), and photopolymerization (44) to explore and analyze various chemical phenomena by utilizing optical force. The results for single MPs and single microdroplets based on optical trapping were summarized by our research groups (45, 46) and then Ashkin (47, 48) introduced the research area called optical trapping–based microchemistry.

In optical manipulation, the smallest target is atoms, and indeed, atom trapping is made possible by laser cooling (49). For the nanometer-sized targets between MPs and atoms, various kinds of molecules and nanomaterials have been widely studied; typical examples are molecular clusters (50–53), aggregates (54, 55), polymers (56–61), supramolecules (62–64), DNA molecules (65), carbon nanotubes (66, 67), micelles or vesicles (68–70), quantum dots (71–73), nanodiamonds (74), nanowires (75–77), polymer nanoparticles (NPs) (78, 79), and metal NPs (80–85). In this review, these targets are called generally referred to as NPs. To provide background for this discussion, we first summarize the theoretical framework for how mechanical force is loaded onto NPs based on Rayleigh scattering and point-dipole approximation (86).

When the radius of an NP is sufficiently smaller than the wavelength of the laser, this approximation can be used to describe the behavior of the NP in an electromagnetic wave. An NP is treated as an induced, simple point dipole, and optical force is exerted on this dipole. The force can be divided into two components: a scattering force component (F_{scat}) and a gradient force component (F_{grad}). The scattering force is associated with the momentum change of the electromagnetic wave. Upon laser irradiation, light scattering is induced by the dipole, and the moment of the incident light is transferred to an NP. Due to this momentum change, the scattering force (F_{scat}) is exerted on an NP. This force is given by the equation

$$F_{scat}(r) = \frac{C_{scat} \cdot \langle S(r,\ t)\rangle_T}{c/n_2}, \qquad 1.$$

where n_2 is the refractive index of a surrounding medium, c is the speed of light in a vacuum, C_{scat} is the scattering cross section of an NP, and $\langle S(r,t)\rangle_T$ is the time-averaged Poynting vector at position r. When the radius of the NP (a) is used, the scattering force increases in proportion to a^6.

The gradient force is associated with a Lorentz force that acts on a dipole located in an inhomogeneous electromagnetic field. The gradient force that an NP experiences in a steady state is given by

$$F_{grad}\,(r) = \pi {n_2}^2 \varepsilon_0 a^3 \left(\frac{m^2-1}{m^2+2}\right) \nabla |E\,(r)|^2, \qquad 2.$$

where ε_0 is the dielectric constant in the vacuum, m is the relative refractive index of the NP, and $E(r)$ is the electric-field vector. The intensity of the laser, $I(r)$, is defined as

$$I(r) = \frac{1}{2} n_2 \varepsilon_0 c |E(r)|^2. \qquad 3.$$

Given this definition, the gradient force is then calculated in terms of the intensity distribution of the beam by

$$F_{grad}(r) = \frac{2\pi n_2 a^3}{c} \left(\frac{m^2-1}{m^2+2}\right) \nabla I(r). \qquad 4.$$

Considering the relationship between force and potential, the optical potential energy well is described by

$$U_{grad}(r) = -\frac{2\pi n_2 a^3}{c} \left(\frac{m^2-1}{m^2+2}\right) I(r). \qquad 5.$$

Different from the scattering force, the gradient force is proportional to a^3. In an optically evolved phenomenon, assembly size increases with time so that the balance between the scattering force and gradient force is dynamically changed.

The optical forces that are exerted on MPs consist of gradient and scattering forces. When the gradient force is larger than the scattering force, optical trapping is possible. This is generally true in bulk solution; however, the situation is different at liquid/air, liquid/liquid, and liquid/solid interfaces, where the scattering forces toward the interfaces can also immobilize the object. Thus, even small objects can be trapped at an interface with relatively weak gradient forces, leading to new optical assembling phenomena.

We usually use a 1,064-nm CW laser as a trapping light source, as its long wavelength tends to hamper multiphoton excitation of the trapping targets. NPs are much smaller than the focal area, so a number of NPs can be confined in a given potential. The NPs physically and chemically interact with one another, producing various phenomena under optical trapping. As the local concentration of NPs in the confined potential increases above a certain level, association, aggregation,

cluster formation, and even nucleation can be induced. The range of phenomena produced can be expanded. If the trapping laser light is absorbed by solvent molecules through their vibrational overtone mode, the local temperature becomes elevated. For example, an elevation of 22 K per 1 W of laser power is estimated for 1,064-nm laser trapping in aqueous solution (87). The temperature distribution is wider than the focal volume due to thermal conduction. Therefore, a thermal phase transition that starts at the focus expands into the area where the temperature is high. In these cases, the optical potential only triggers the phenomena, and the assembly expands outside of the focus following thermodynamic conditions determined by temperature, concentration, and other factors.

At the surface and interface, the trapping laser at the focus is strongly scattered by the trapped NPs and is propagated through the gathered NPs, forming an attractive potential at their edge. The multiple scattering results in a decrease in the laser's intensity; however, a small gradient force is usually enough to immobilize the NPs. Also, the scattering force pushes NPs toward the surface and interface, contributing to their immobilization. As a result, a single assembly of NPs can grow to become much larger than the focus along the solution surface and interface. In the past decades, we have demonstrated various interesting phenomena that we call optically evolved assembling, and we have been elucidating their dynamics and mechanisms that are characteristic of solution surface and solution/glass interfaces.

In this review, we mainly summarize our seminal research and discuss the evolved trapping of molecules and NPs at solutions and interfaces. Our viewpoint for comprehensively understanding their dynamics and mechanisms is based on optical trapping potential expansion by nonlinearly evolving interactions between the trapping laser and the NPs. The Gaussian beam potential is tightly focused on a solution surface and interface where a single NP is trapped (**Figure 1*a***). When the NP concentration of the mother solution is high, many NPs are confined, triggering cluster formation, crystallization, and crystal growth of molecules as well as phase transition of the polymer solution, phenomena that are similar to those observed under conventional thermodynamic conditions. In the case of low solute concentration, the trapping potential does not change much. The advantage of optical trapping is its high spatiotemporal controllability. When the trapping laser light is scattered by the trapped NPs at a surface and interface, the laser propagates through the trapped NPs and they interfere with one another, expanding the optical trapping potential. Optically evolving crystallization, periodic arrangement of polystyrene (PS) NPs, and the assembly and swarm of Au NPs, which are never observed in solution, are illustrated in **Figure 1*b–d***, respectively. In the following sections, we present how new molecular and NP phenomena are induced at a solution interface by optical force, propose their dynamics and mechanisms, and describe possible applications.

2. CHEMICALLY EXPANDING ASSEMBLY OF MOLECULES AND POLYMERS IN SOLUTION

Under the optical conditions in our group's experiments, the effective focal volume is diffraction limited so that the attractive potential size is about 1 μm. Conventional organic molecules and inorganic compounds are small, so the exerted optical force is weak and does not stop vigorous Brownian motion in solution at room temperature. Their movement is just slowed down, which is called biased diffusion (88–90). Our optical trapping experiments have shown that a few nanometers and 20 nm are the necessary diameters for metal and organic NPs, respectively. One example is shown in **Figure 2*a*** (58), in which polymers were trapped at a focus and aggregated with each other, producing a single assembly. The assembly, which was saturated by radiation, was about 1 μm in size, similar to its focal volume. In this case, the gradient force overcame the scattering

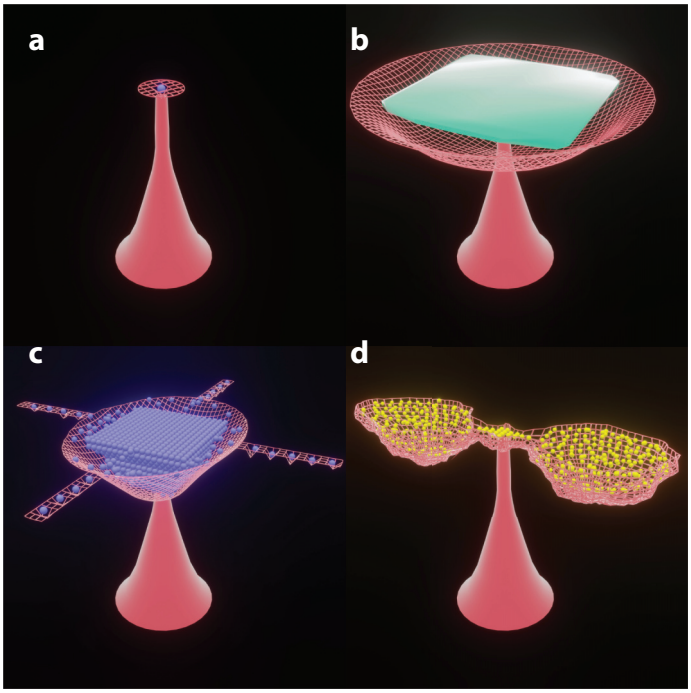

Figure 1

Illustrations of optically evolved assembly. The modification of optical potential and the expansion of the distribution of molecules and nanoparticles (NPs) are induced by interactions between the trapping laser and the NPs. (*a*) A single NP at a solution surface, (*b*) a single crystal of L-phenylalanine at a solution surface, (*c*) a single assembly of polystyrene (PS) NPs with hornlike elongated linear aggregates at a solution/glass interface, and (*d*) Au NPs at a solution/glass interface. As NPs are distributed only below the solution surface and interface, the top of each illustration is flat. The focal volume of the 1,064-nm trapping laser is approximately 1 μm^3, while the optically evolving molecular crystal shown in panel *b*, the periodic arrangement of PS NPs with four horns in panel *c*, and the two swarms of Au NPs in panel *d* reach a few tens of micrometers.

force in the focal volume; however, for a larger trapped aggregate, the scattering force can be stronger than the gradient force. In the latter case, the aggregate was then ejected from the focus. This is one reason why an assembly in solution usually has a size similar to that of the focal volume. This behavior is quite common in solutions and has been systematically confirmed for poly(*N*-isopropylacrylamide) (PNIPAM) and its family (56, 57).

The 1,064-nm trapping laser excites the overtone vibrational mode of H_2O, leading to local laser heating (87) and subsequent thermal conduction. In the case of PNIPAM in aqueous solution, the polymer changes from random coil to globule conformation with prolonged irradiation, exhibiting a sol–gel phase transition. Indeed, one assembly observed at the focus reached a size of 10 μm, much larger that the focal volume, reflecting the heated area (56). To monitor the local structures of polymers, pyrene-labeled PNIPAM (Py-PNIPAM) was studied, as shown in **Figure 2*b*** (57). Dimer fluorescence around 480 nm reflects a high local concentration of dimer configurations in the ground state, while the vibrational structure of pyrene fluorescence indicates local polarity. Both photothermal and optical trapping effects determine the assembly structure in H_2O, but the former effect is hampered in D_2O and the characteristic spectral change indicates strong packing of PNIPAM by optical trapping.

Another example shown in **Figure 2*c*** is the formation of ordered fibril- and particle-like assemblies during the solvent evaporation process on a glass substrate (60). This is achieved by combining laser irradiation with convection flow in the cast solution. When the viscous drag of the solution in the convection is stronger than the optical force, fibril-like assemblies can form. The molecular orientation in these assemblies differs from that in self-assembled fibril-like structures, and such orientation can be controlled by the polarization direction of the focused laser

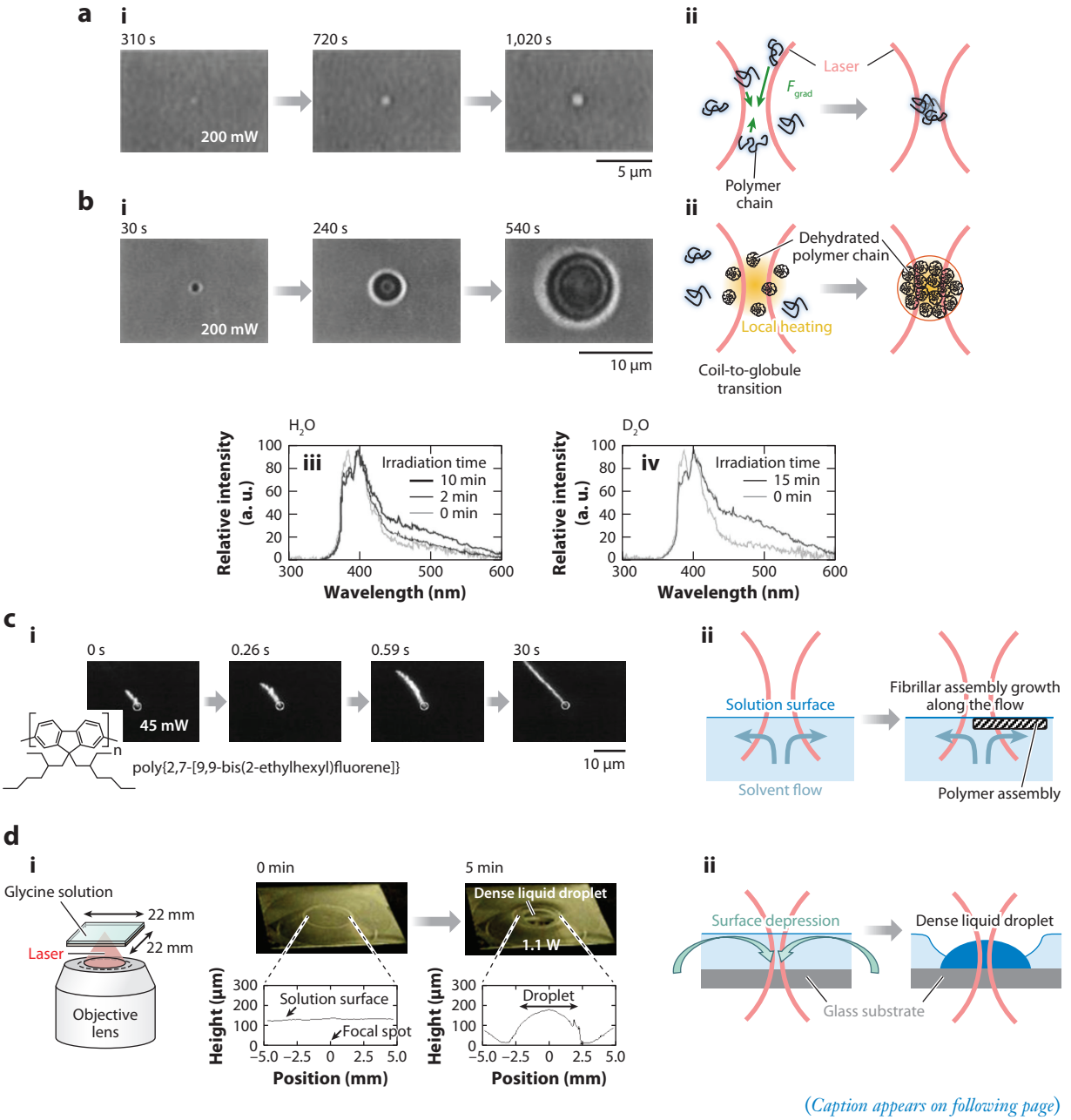

(*Caption appears on following page*)

Figure 2 (*Figure appears on preceding page*)

Optical trapping and assembling phenomena coupled with thermal effects. (*Left*, *i*) Illustrations of the experiments. (*Right*, *ii*) Schematic illustrations of respective laser trapping behaviors. The laser power is given in corresponding optical images. (*a*) Laser trapping behavior of poly(*N*-vinylcarbazole) in *N*,*N*-dimethylformamide. (*i*) Optical transmission micrographs around the focal spot, showing a particle-like molecular assembly. Panel *a* subpanel *i* adapted with permission from Reference 58; copyright 1998 American Chemical Society. (*b*) Fluorescence analysis of laser trapping of pyrene-labeled poly(*N*-isopropylacrylamide) in H_2O and D_2O. (*i*) Optical transmission micrographs around the focal spot in H_2O, producing (*ii*) a large molecular assembly due to photothermal effects. (*iii*, *iv*) Normalized fluorescence spectra, which were obtained by laser trapping in (subpanel *iii*) H_2O and (subpanel *iv*) D_2O solutions, are shown at the different irradiation times. Panel *b* subpanels *i*, *iii*, and *iv* adapted with permission from Reference 57; copyright 1997 American Chemical Society. (*c*) Laser trapping behavior of poly{2,7-[9,9-bis(2-ethylhexyl)fluorene]} in tetrahydrofuran. (*i*) Fluorescence images and (*ii*) illustrations show the fibril-like assembly growing along the solvent flow. The chemical structure of the polymer is given in the inset to subpanel *i*. Panel *c* subpanel *i* adapted with permission from Reference 60; copyright 2007 American Chemical Society. (*d*) A millimeter-scale dense liquid droplet of glycine (23 wt%) formed under focused laser irradiation of a thin film of the D_2O solution. (*i*, *Top*) Optical micrographs are shown of the sample and (*bottom*) the corresponding solution surface profiles before and after irradiation. Panel *d* adapted with permission from Reference 95; copyright 2012 American Chemical Society.

beam. When the viscous drag of the convection solution is weak, particle-like assemblies form in which polymer orientation is still controllable by the polarization direction of the trapping laser.

Heat generated at the focal spot diffuses to the surroundings, and surface tension decreases with increasing temperature. Due to the resultant inhomogeneous distribution of surface tension, the solution surface becomes depressed around the laser focus (91, 92), leading to the formation of an ultrathin film just a few micrometers in thickness. In parallel, convection flow transports solutes to the depressed area upon which optical force is acting (93). As a result, the efficient optical trapping of transported solutes is achieved, and the local solute concentration quickly increases, resulting in nucleation for liquid–liquid phase separation (LLPS). In fact, a dense liquid droplet is formed through phase separation in a thin film of a supersaturated D_2O solution of glycine (94, 95). Liquid nucleation takes place after the surface depression occurs, and the liquid nucleus grows increasingly larger by absorbing solutes from the surrounding solution. As shown in **Figure 2*d***, the droplet takes on a thin convex shape with a diameter of 5 mm, which is 5,000× larger than the focal spot (about 1 μm in diameter). The saturation degree of the droplet is 2.7, but it remains a liquid without crystallization under laser irradiation. Similar droplet formation is observed for other amino acids, potassium chloride, and urea. As introduced in **Figure 2*b*–*d***, optical trapping occasionally accompanies thermal effects, such as the phase transition of polymers, convection flow, and surface deformation, through which a unique molecular assembly with a size much larger than that of the focal volume is formed in a spatially and temporally controlled manner.

3. OPTICALLY EVOLVING CRYSTALS AT THE SOLUTION SURFACE

During laser trapping at a solution surface, molecular or ionic crystals are formed at the focal spot. This crystallization was first demonstrated for glycine in 2007 (96). Since then, it has been observed for other amino acids (97–105), potassium chloride (106), sodium chlorate (107), and lead halide perovskites (108, 109). Laser trapping locally and transiently increases the concentration of solutes not only at but also around the focus. Therefore, crystallization can be induced even in an unsaturated solution. A representative example is given in **Figure 3*a*** (101). The trapping laser was focused onto the surface of an unsaturated solution of L-phenylalanine (L-Phe). The initial solution has a saturation degree of 50%, a situation that never exhibits spontaneous crystallization. After several minutes of irradiation, crystallization is induced at the focal spot. The resultant plate-like L-Phe crystal is stably trapped at the focus and continuously grows larger. This crystal growth pauses when the laser power is decreased to one-twentieth of the original value. The crystal is stably trapped even at this low laser power but starts to dissolve after a certain amount of

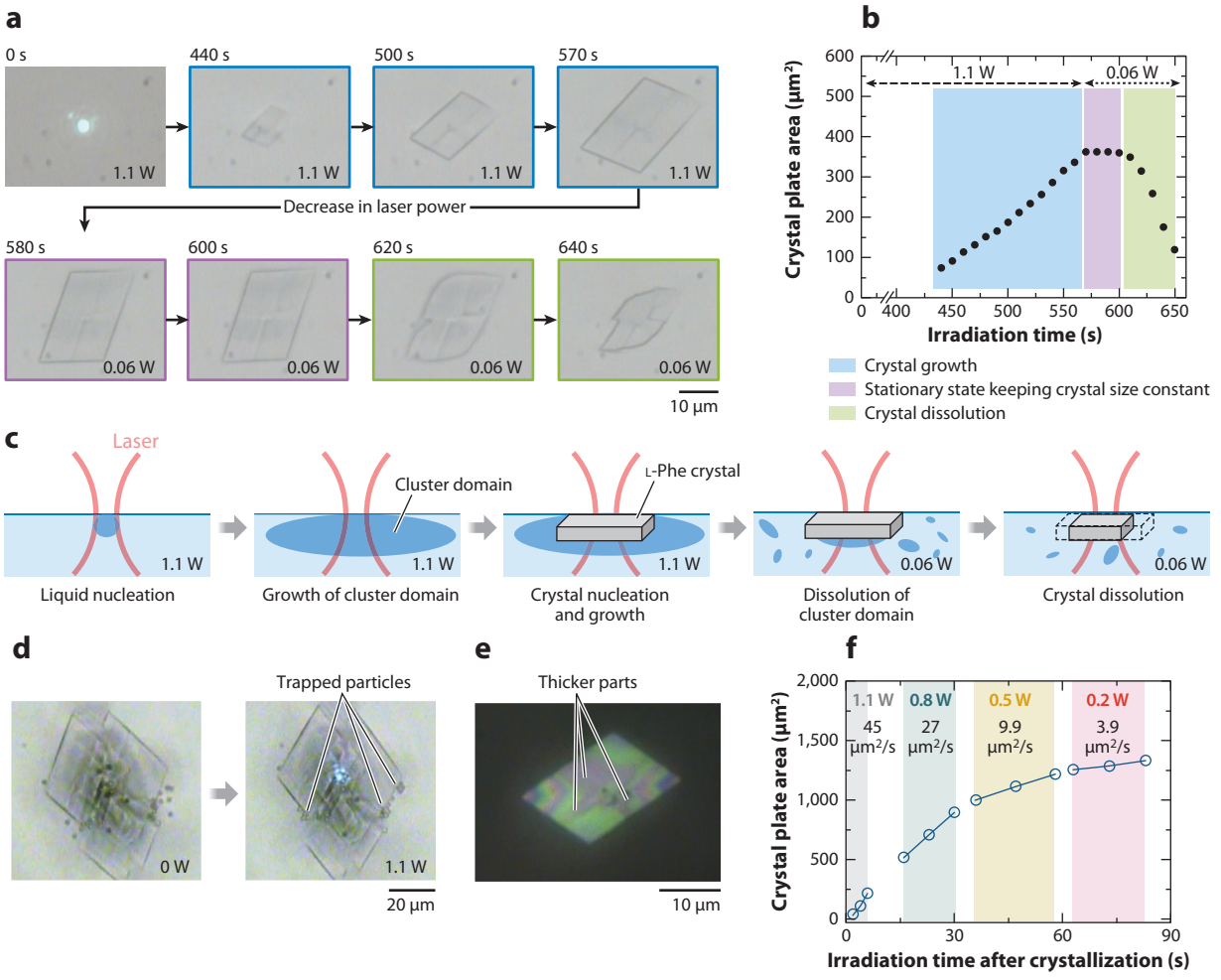

Figure 3

Laser trapping–induced crystallization of L-phenylalanine (L-Phe) in H_2O. (*a*) Optical transmission micrographs around the focal spot and (*b*) a graph of time evolution of the crystal plate area during laser trapping at the air/solution interface. Panels *a* and *b* adapted with permission from Reference 104; copyright 2018 American Chemical Society. (*c*) A schematic illustration of laser trapping dynamics at 1.1 and then 0.06 W. (*d*) Optical micrographs of particles around an L-Phe crystal. Panel *d* reproduced with permission from Reference 101; copyright 2013 American Chemical Society. (*e*) An optical reflection image of an L-Phe crystal. Panel *e* reproduced with permission from Reference 105; copyright 2019 The Japan Society of Applied Physics. (*f*) A graph showing the temporal change in the crystal plate area upon the step-by-step decrease of laser power. The 2D crystal growth rate at each laser power is shown. Panel *f* adapted with permission from Reference 103; copyright 2016 American Chemical Society.

time (**Figure 3*a*,*b***). The stationary state keeping crystal size constant can be explained by assuming a highly concentrated area of solute around the crystal (**Figure 3*c***). This dense area gradually diffuses into the surrounding solution during the laser irradiation at low power. As a result, the surrounding solution is homogenized, and the crystal is exposed to the unsaturated solution, initiating crystal dissolution. Indeed, the crystal quickly dissolves when it is optically manipulated to a position far from the original focal spot. The size of the highly concentrated area was estimated by the optical manipulation experiment to be a few tens of micrometers.

The mechanism of formation of a highly concentrated, large area of L-Phe may be similar to that of the dense liquid droplet of glycine (**Figure 3*c***). L-Phe liquid-like clusters, in which solute and solvent molecules are associated with weak interactions, are attracted by optical force and merge with each other, forming larger clusters. Through this process, the optical potential becomes increasingly deeper, and the local concentration is gradually increased. As a result, liquid nucleation takes place at the focal spot. While being irradiated, the resulting liquid nucleus is more energetically favorable than the surrounding solution and so enlarges through spontaneous growth. We call the dense area a cluster domain, as it is formed by the association of L-Phe liquid-like clusters. Actually, two order parameters and a concentration of solutes with their associated structures are known to be necessary for crystallization. Before crystallization, the optical potential forms only at the focal spot, and the shape of the potential reflects the intensity distribution of the incident laser beam. In contrast, the optical potential is spatially modified after crystallization, as illustrated in **Figure 1*b***. The potential is extended to the outside of the focal spot, which enables optical trapping at the edge of the crystal.

The expansion of optical potential is visually confirmed by trapping PS MPs with a diameter of 1 μm. Upon focused laser irradiation, the MPs gather at the edge of an L-Phe crystal. The MPs are closely arranged at the crystal edge, although they are not directly irradiated by the laser (**Figure 3*d***). After switching off the laser, the gathered MPs start to diffuse into the surrounding solution, meaning that the particles are transiently attracted by the laser irradiation. This remote trapping at the crystal edge can be explained by an optical mechanism. The laser light sent into the center of the crystal propagates inside the crystal outward from the focus and forms an optical potential at the crystal edge. This extended optical potential attracts MPs to the crystal from the surrounding solution. Similarly, L-Phe in a surrounding cluster domain is also trapped at the crystal edge, which leads to continuous crystal growth even in the unsaturated solution. The mechanism of light propagation is supported by the observed framework-like structure of the crystal. We investigated the crystal growth behavior of L-Phe with reflection microscopy under laser trapping conditions. L-Phe crystals appear to be colored in reflection micrographs due to the interference of white light being reflected at the upper and lower crystal faces. The interference is strongly dependent on crystal thickness, so the inhomogeneity of crystal thicknesses is visualized. We found that a framework-like structure with a wider thickness is formed from the focus toward the crystal edge (**Figure 3*e***). This structure likely acts as a waveguide to propagate the laser outward from the focal point, and the propagated light modifies the optical potential, enabling the optical trapping of L-Phe and MPs at the crystal edge. How L-Phe molecules are trapped and concentrated at and around the focus is dependent on the power of the laser. Thus, the 2D growth rate of plate-like L-Phe is slowed down by a decrease in the input laser power (**Figure 3*f***). Therefore, crystal growth can be optically controlled by tuning the laser power.

4. OPTICALLY EVOLVING ASSEMBLY OF POLYMER NANOPARTICLES AT THE SOLUTION SURFACE

The optical assembly of PS NPs is itself an interesting topic in colloid science and technology and is also considered to be a useful reference for the optically evolving crystallization of molecules. In the case of 200-nm PS NPs at a solution surface (110), a disklike assembly is formed and continuously grows, keeping a circular shape during the irradiation as shown in **Figure 4*a***. The trapping laser seems to gather NPs, propagate through the formed NP assembly, and expand the trapping potential further, thus growing the aggregates outward at the solution surface. NPs confined in focal volume induce the scattering of the trapping laser, and the surrounding NPs propagate the scattered laser, forming a potential just outside the circular assembly. PS NPs are trapped in the

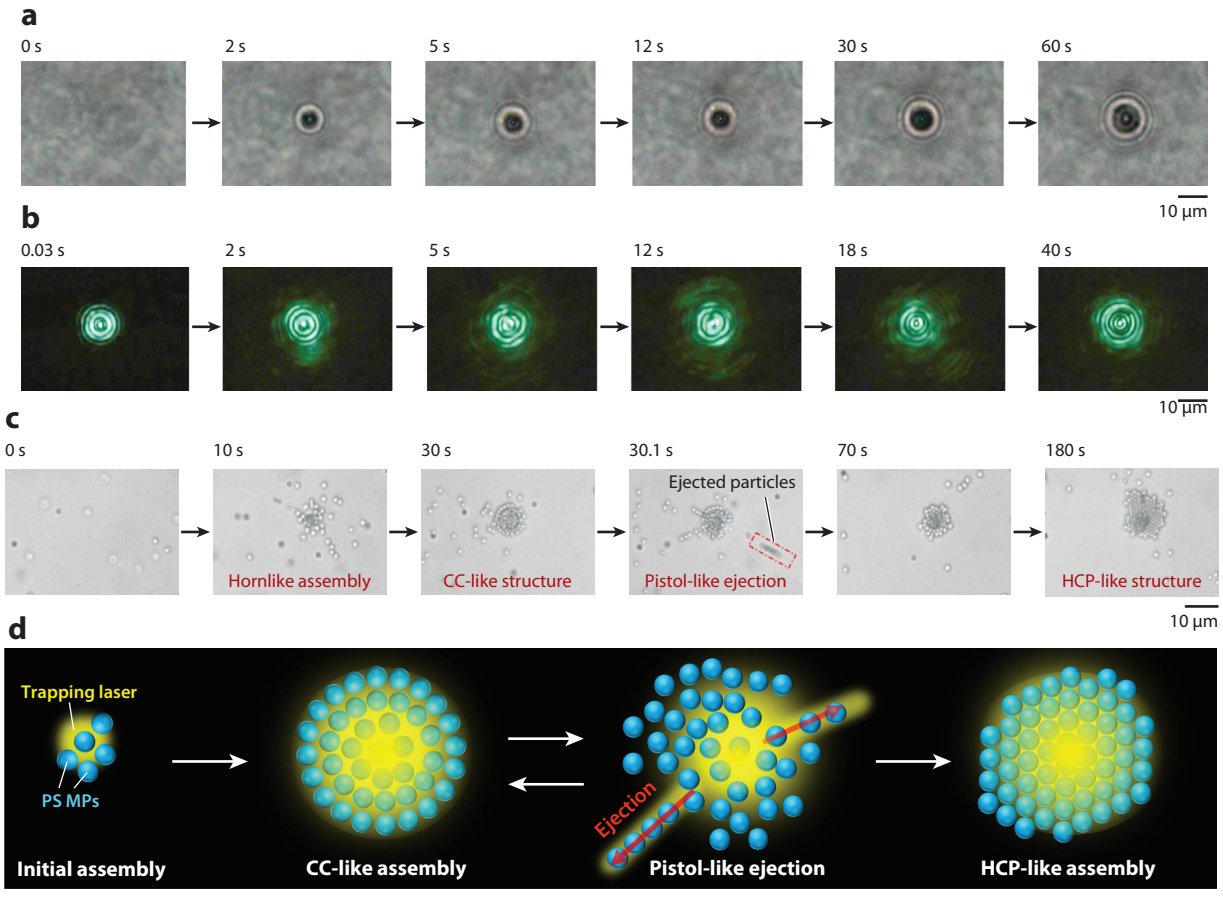

Figure 4

(*a*) Optical transmission micrographs and (*b*) backscattering images from the optical trapping of 200-nm PS NPs at an aqueous solution surface after switching on the trapping 1,064-nm laser. Panels *a* and *b* adapted with permission from Reference 110; copyright 2016 American Chemical Society. (*c*) Optical transmission micrographs and (*d*) a schematic illustration for the optical trapping–induced assembly and rearrangement of 1-µm PS MPs at a D_2O solution surface. Hornlike assembly, CC-like structure, pistol-like ejection (outlined by *red rectangle*), and HCP-like structures are indicated in corresponding images. Panels *c* and *d* adapted with permission from Reference 111; copyright 2020 American Chemical Society. Abbreviations: CC, concentric circle; HCP, hexagonal close-packed; MP, microparticle; NP, nanoparticle; PS, polystyrene.

potential, increasing the circular assembly size. This optically evolved assembling proceeds until the formed optical potential becomes shallow, comparable to the thermal energy of NPs. To confirm this idea, we monitored the backscattering pattern from the assembly. **Figure 4*b*** shows the time evolution of the backscattering images from the 1,064-nm trapping laser, in which the concentric circle (CC) pattern extends continuously and symmetrically into the surrounding solution. The growth of the circular shape of backscattered light corresponds well to the images shown in **Figure 4*a***.

How intense laser irradiation traps NPs and MPs at the focus in a solution has been studied by many groups, but it is not widely accepted that optical force is useful for forming a large disk-like assembly of molecules and NPs at the solution interface. To visualize the trapping assembly dynamics, we have sampled 1-µm PS MPs (111). When the 1,064-nm laser is focused, the MPs

gather far from the focus, leading to the formation of a single large assembly with CC-like packing. The assembly evolves with the irradiation time, exhibiting an increase in lateral size, producing the pistol-like ejection of several MPs in a linearly aligned manner, rearranging to another CC-like assembly, and eventually forming a hexagonal close-packed (HCP) structure of PS MPs. Representative sequential transmission optical micrographs are shown in **Figure 4*c***. The CC-like structure is considered to be kinetically prepared, while the 2D HCP structure is thermodynamically favored at the interface (112, 113). This is an experimental model of what happens microscopically at the solution surface upon optical trapping. The behavior presently observed with continuous irradiation is illustrated in **Figure 4*d***.

Pistol-like ejection is always induced radially from the center to the outside, so we think that the light scattering and propagation of the trapping laser inside the CC assembly has an important role in this process. Occasionally, we observed that the 1-μm PS MPs were radially extended, forming a line, and then they were ejected. This occurred along the scattering lines of the trapping laser from the focus, as similarly observed for 200-nm PS NPs at the solution surface (114) and for 500-nm PS NPs at the solution/glass interface (115). Here the 1-μm PS MPs in the line were ejected when the incoming MPs collided with the assembly, as illustrated in **Figure 4*d***. We observed that the laser scattering always looked like multiple radial white streams expanding from the center of the CC-like structure. This supports our idea that the scattered light of the trapping laser from the central part of the CC-like assembly and its directional propagation through the structure is the origin of pistol-like ejection at the solution surface. Quantitative analysis of pistol-like ejection is being performed; for example, the ejection speed for the highest laser power (1.4 W) was estimated to be 200 μm/s, and the ejection angle was tilted by 11–15° from the solution surface.

5. OPTICALLY EVOLVING ASSEMBLY OF POLYMER NANOPARTICLES AT THE SOLUTION/GLASS INTERFACE

Light scattering and propagation of the trapping laser are critical for molecular crystallization and disklike assembly formation of NPs, which is directly demonstrated by the periodic assembly formation of 500-nm PS NPs at the solution/glass interface (**Figure 5*a***) (115). Compared to that with the solution surface, the interface with glass is rigid, so PS NP packing is more stable, leading to an arrangement that allows more efficient scattering and propagation of the trapping laser. The single lateral assembly is deformed and becomes elongated along the linear polarization direction of the trapping laser. This is due to the high numerical aperture of the objective lens used. For the circularly polarized laser, the assembly shape is circular. A long period of irradiation with a linearly and circularly polarized laser produces elongated and circular assemblies with four and six horns at their edges, respectively. The packing structure at the center determines the expanding assembly shape by propagating the trapping laser. The tetragonal and hexagonal packing structures at the assembly center, which correspond to four and six horns, respectively, are monitored by diffraction pattern measurement, as shown in **Figure 5*b***. In addition, **Figure 5*c*** shows the transmission spectra for four and no horns, which agree well with the images of these structures. This polarization-dependent assembly is well explained by theoretical calculation of the laser beam profiles at a focal plane. The calculated profiles in **Figure 5*d*** match the shapes of the corresponding NP assemblies, so the PS NPs seem to be arranged according to the trapping laser intensity distribution. The results confirm that propagation of light from the trapping laser through packed PS NPs yields the horns, which is illustrated in **Figure 1*c***. This mechanism has great potential for assembling and fabricating fascinating materials.

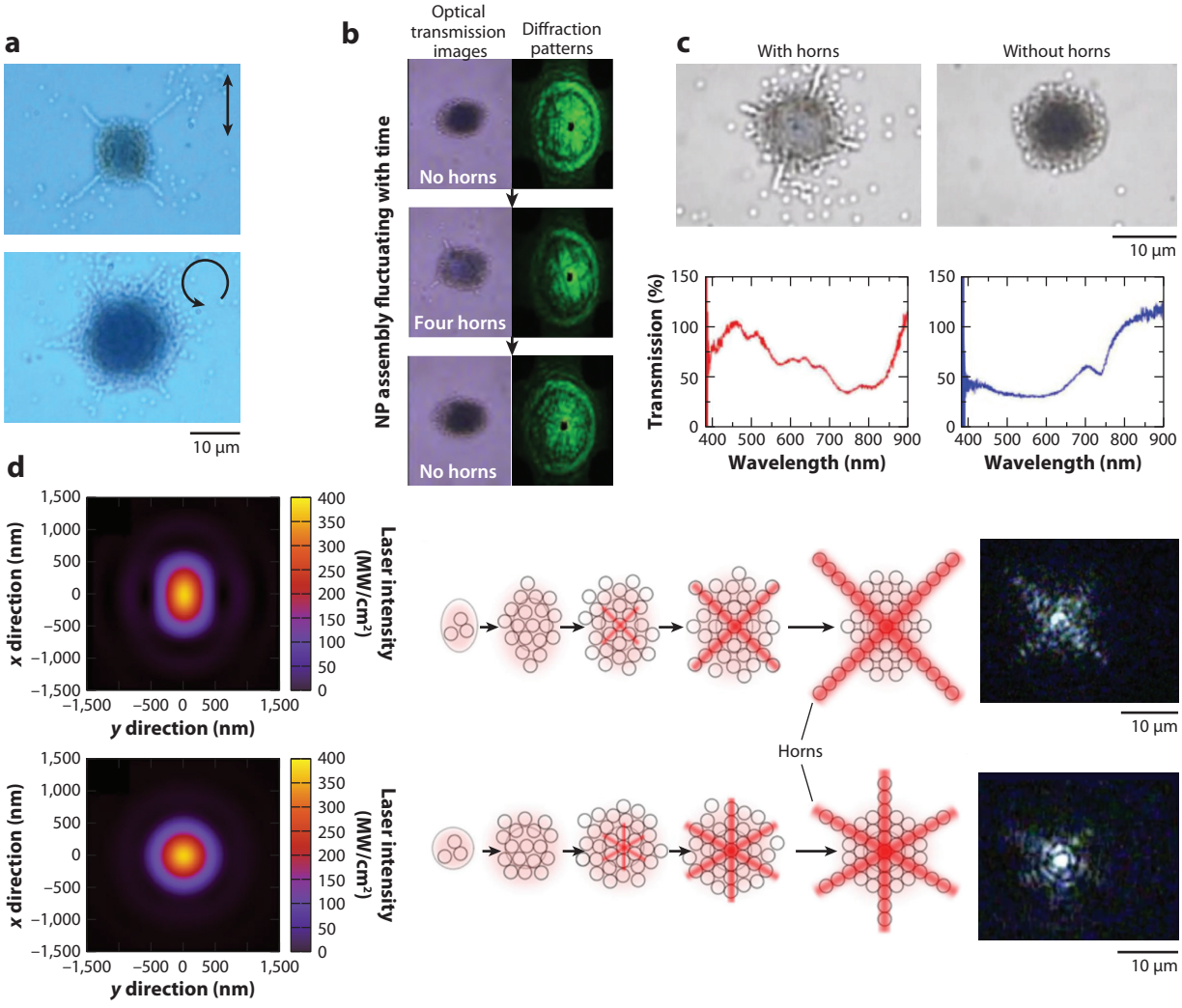

Figure 5

(*a*) Optical transmission micrographs of the optical trapping of 500-nm polystyrene (PS) nanoparticles (NPs) at an aqueous solution/glass interface. (*Top*) Linearly and (*bottom*) circularly polarized lasers produce four and six hornlike structures, respectively, at the edges of the single disklike assemblies. The polarization is shown by straight and circular black arrows. (*b*) Temporal changes in optical transmission micrographs and diffraction patterns of the optical trapping of 500-nm PS NPs at an aqueous solution/glass interface with the linearly polarized laser. (*c*) Optical transmission micrographs of NP assemblies (*left*) with horns and (*right*) without horns and the corresponding transmission spectra measured at the focus. These assemblies are formed at different times during the optical trapping of 500-nm PS NPs at an aqueous solution/glass interface with a linearly polarized laser. (*d*, *left*) Images and illustrations showing the spatial distribution of calculated laser intensity with a high–numerical aperture lens for linearly and circularly polarized lasers. (*Middle*) Schematic illustrations showing assembly growth of 500-nm PS NPs with (*top*) tetragonal and (*bottom*) hexagonal structures for linearly and circularly polarized trapping lasers, respectively. The trapping laser propagates along the structures, producing either four or six horns. (*Right*) Backscattering images of the trapping laser observed from the assembly. Images in panels *a* and *d* reproduced with permission from Reference 115; copyright 2016 American Chemical Society.

6. OPTICALLY EVOLVING SWARMING OF GOLD NANOPARTICLES AT THE SOLUTION/GLASS INTERFACE

Recently, we have extended these experiments at the solution/glass interface to gold (Au) NPs, and we have found a new phenomenon that is characteristic of their inherent surface plasmon resonance (SPR) (116). The heavy 200-nm Au NPs sink to the bottom of the sample but are lifted upward upon trapping laser irradiation, as shown in **Figure 6*a***. Initially, a few Au NPs are trapped at the focal spot at the interface and efficiently scatter the trapping laser light. With linearly polarized laser irradiation, dipolar scattering of Au NPs renders the light distribution perpendicular to the direction of laser polarization. The scattered light expands the optical potential and collects more Au NPs at both sides of the assembly outside the focal spot (**Figure 6*b***). The NPs fluctuate as a group like flying bees and form a dumbbell-shaped assembly of about $5 \times 10\ \mu m^2$ at the solution/glass interface. In the case of circularly polarized laser irradiation (**Figure 6*c***), the

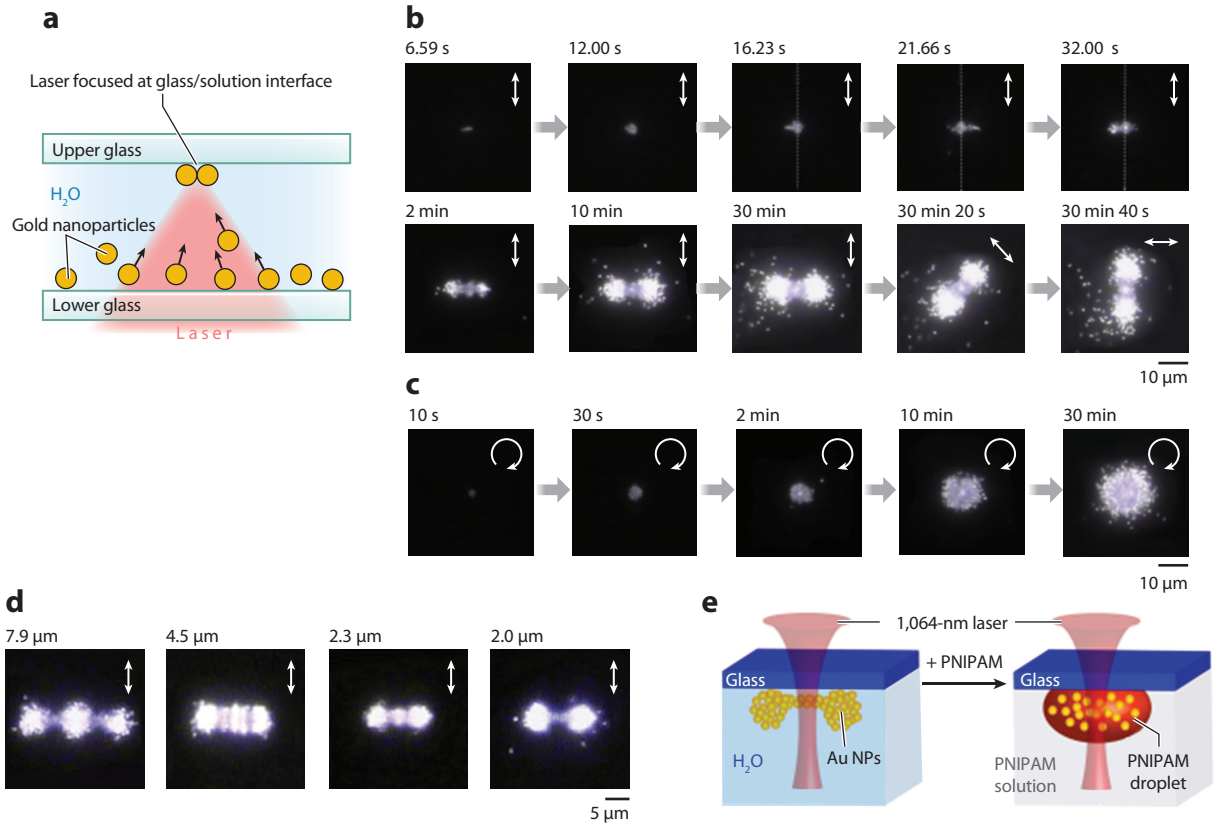

Figure 6

(*a*) A schematic illustration of the optical trapping and swarming of 200-nm Au NPs at an aqueous solution/glass interface. Au NPs sink to the bottom of the sample cell and are then lifted up by trapping laser irradiation. (*b*,*c*) Temporal change in light-scattering images showing the optical trapping or swarming of Au NPs with a linearly (panel *b*) or circularly (panel *c*) polarized laser. Panels *b* and *c* adapted with permission from Reference 116; copyright 2018 American Chemical Society. (*d*) Light-scattering images of Au NP trapping and swarming using two linearly polarized trapping laser beams of equal power. The distance between the centers of the two laser beams is given in the images. (*e*) Schematic illustrations of Au NPs first swarming and then stopped in a single microdroplet of PNIPAM, which is prepared by local phase transition due to photothermal heating of the NPs. Abbreviations: NP, nanoparticle; PNIPAM, poly(*N*-isopropylacrylamide).

trapping laser expands isotopically in all directions, and consequently a circular swarming assembly is formed. The Au NPs undergo vigorous fluctuation, and back-and-forth movement between left and right swarms is observed. Multiple scattering among multiple NPs must be intrinsic, and the position of NPs can be replaceable, that is, one NP can be replaced with another. To demonstrate this characteristic, we split the trapping laser into two and manipulated the NPs freely with a Galvano mirror. **Figure 6*d*** shows that the number of swarms and the distance between them can be controlled by changing the distance between the foci of the two trapping lasers.

Au NPs efficiently scatter the trapping laser, which leads to larger NP swarms when the laser wavelength matches the SPR band (117). In the beginning of this section, we described the results of trapping 200-nm Au NPs with a 1,064-nm laser. Under the same conditions, the swarm is not found when the diameter of the NPs is smaller than 200 nm. The SPR band shifts to a shorter wavelength when the Au NP size decreases; as a result, the 1,064-nm laser becomes off-resonance for the smaller NPs. In other words, the swarming assembly for smaller Au NPs should be observed if the laser wavelength is shifted toward the SPR band. Of course, a larger swarm could be achieved if the wavelength is exactly resonant to the SPR band. Optically evolved assembling and swarming are considered to be complex behaviors, and a large number of Au NPs interact with each other through attractive multiple light scattering and electrostatic repulsion, which expands the effective optical trapping potential, as illustrated in **Figure 1*d***. Brownian motion, hydrodynamic interaction, and thermal heating must be coupled with the swarming (118); however, the swarming surely starts from the scattered light of Au NPs, and matching the trapping laser with the SPR band is critical.

In general, heating and convection induced by the laser irradiation of Au NPs have been extensively studied (119, 120), and these modes should be involved in the present assembly and swarming phenomena. One important issue to examine is how the dumbbell-shaped swarm depends on the heating and convection caused by irradiation of Au NPs. We designed an experiment to add PNIPAM to an aqueous solution of Au NPs. As mentioned previously, this polymer is soluble in water but undergoes LLPS above its lower critical solution temperature (32°C) (121, 122). This behavior is locally achieved by irradiating a single Au NP under a microscope (123, 124). In the case of Au NPs in PNIPAM solution, trapping, local heating, and local LLPS develop simultaneously, as they are coupled with each other (118). The Au NPs are embedded in the prepared droplet of PNIPAM and no longer show swarming, as illustrated in **Figure 6*e***. The observation and analysis of such dynamically evolving processes provide information on the morphology and sizes of swarms and assemblies.

7. MECHANISM AND APPLICATION OF OPTICALLY EVOLVED ASSEMBLING AT SOLUTION SURFACES AND INTERFACES

We have described the optical force–induced assembling phenomena of molecules and NPs at solution surfaces and interfaces, showing that the assembly size is much larger than the focus. Our proposed mechanism is supported by direct observation of light scattering and propagation of the trapping laser, and we know that surface tension, convection flow, and thermophoretic effects (125–127) are all involved to various degrees. We plan to integrate all possible dynamics and mechanisms to enable a comprehensive understanding of this process. Here we introduce our recent results on the optical trapping and assembling of 100-nm PS NPs at the solution surface and point out a new possible mechanism. Upon irradiation of a 1-μm focal spot, we found a single large, disklike assembly a few tens of micrometers in diameter around the spot (**Figure 7*a***). Apparently, this assembly is similar to that produced by 200-nm PS NPs; however, needlelike structures expanding radially out of the focus are also formed (128). After switching off the trapping laser,

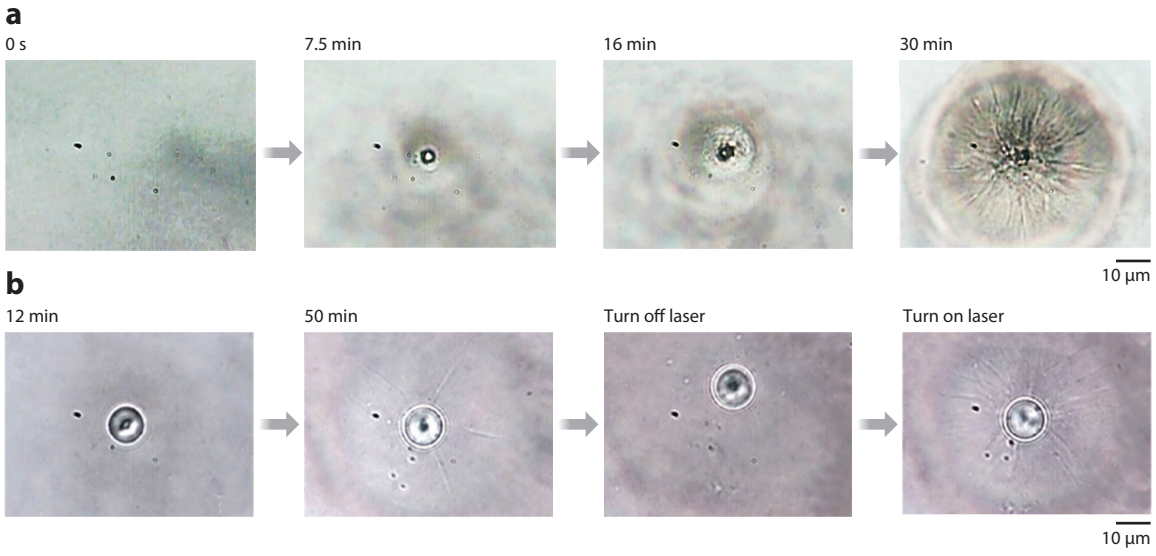

Figure 7

(*a*) Optical transmission micrographs of the optical trapping of 100-nm polystyrene (PS) nanoparticles (NPs) at an aqueous solution surface. (*b*) Optical transmission micrographs of the optical trapping of 100-nm PS NPs around an optically trapped 10-μm PS microparticle at the surface of a D_2O solution. Micrographs in figure reproduced with permission from Reference 128; copyright 2020 American Chemical Society.

the assembly dissolves and the needlelike structures disappear while the highly concentrated NP domain slowly dissipates. If the trapping laser is switched on again soon, the domain shifts back toward the focus, the disklike assembly is restored, and even the needles reform.

We have designed a new experiment to hamper the light scattering of the trapping laser from the focus, that is, the optical trapping of 100-nm PS NPs around a single optically trapped 10-μm PS MP at a D_2O solution surface. Surprisingly, a similar disklike assembly of NPs as well as needlelike structures forms outside the large 10-μm PS MP (**Figure 7*b***). A similar behavior is observed when switching on and off the laser sequentially. Most of the trapping light irradiates the big MP while the surrounding area is affected by leaked trapping light. These needlelike structures are similar to a discharge pattern from material after a high voltage is applied to its center. The power of the 1,064-nm trapping laser, which is 1.4 W, is focused onto a small 1-μm^2 area so that the laser fluence is roughly 140 MW/cm^2. This power density may result in an optical Kerr effect in which the optical properties of materials are changed; such changes are conventionally examined by irradiating with a nanosecond to femtosecond laser pulse (129, 130). In our case, CW high-power irradiation may orient phenyl substituents and modify the segment structures inside the PS MP, accompanied by a change in surface charge; consequently, water molecules, being coupled with rearrangement of the 100-nm PS NPs, are dynamically reoriented.

In fact, the assembly of 1-μm PS MPs and the formation of needlelike structures both start at the MP surface. The simulation study reports that the dielectric particles are rearranged in a linear manner under electrical and magnetic fields (131). At the molecular level, these behaviors should be assisted by charge transfer and electron transfer through the hydrogen-bonding network of water molecules. The collected 100-nm PS NPs must be coupled with this network, which induces the electronic polarization of water molecules. We infer that the radially expanding assembly of 100-nm PS NPs may be ascribed to the formation of a giant dipole consisting of water

molecules and the small NPs at the solution surface. The giant dipole and needlelike structures might enable the local electrostatic effect to propagate further than a few tens of micrometers. Such an electrostatic effect may be coupled with the light scattering and propagation.

As previously discussed, optical trapping is usually limited to the area of focus, conventionally about 1 μm^2, but at solution surfaces and interfaces the area affected by irradiation expands into an area with a diameter of a few tens of micrometers, which suggests the great potential of optically evolved assembly in materials applications. The first example of an application is the preparation of a large assembly of MPs, such as our recent successful fabrication of a submillimeter disklike assembly of 20-μm PS MPs with a necklace-like structure of 1-μm PS MPs (132). In the initial solution, 1-μm MPs are homogeneously dispersed in D_2O but 20-μm MPs float on the solution surface due to their having a lesser density than the solvent. Upon trapping a 20-μm MP, 1-μm MPs gather at the surface of the trapped MP and arrange into a circular pattern, forming a necklace-like structure. With further irradiation, more 1-μm MPs are trapped in a concentric manner, producing multiple necklace-like structures at the surface of the 20-μm MP. This hybrid colloidal assembly is shown in **Figure 8*a*** expanding to 150 μm away from the focal spot, although the focal spot diameter is approximately 1 μm as usual. The extension of the optical potential coupled with a specific light propagation mode such as the whispering gallery mode gives us an opportunity to fabricate such a large millimeter-scale assembly with a unique structure.

The second example is the application to lead halide perovskites, a new class of semiconductor materials for next generation optoelectronic devices (108, 133). Optical trapping occurs at the air/solution interface of unsaturated precursor solutions {$MABr/PbBr_2/MACl/PbCl_2$ [MA (methylammonium) = $CH_3NH_3^+$] in a mixture of DMSO (dimethyl sulfoxide)/DMF (dimethylformamide)}. After laser irradiation for a few minutes, a single perovskite crystal ($MAPbBr_{3-n}Cl_n$) is formed at the focal spot. This is due to a local increase in the concentration of perovskite precursors. Indeed, the precursor solutions remain unsaturated after irradiation. Laser trapping of perovskite precursors also enables control of the halide exchange reaction. In the process of trapping MAI (methylammonium iodide) at the surface of a $MAPbBr_3$ crystal, an exchange reaction of $MAPbBr_3$ with iodide ions is induced, and $MAPbBr_{3-n}I_n$, which has a narrower band gap, is formed only around the focal spot. Photoluminescence at the trapping site gradually changes to red from green, while the nonirradiated parts continue to emit green light, as shown in **Figure 8*b***. The optically controlled anion exchange offers a new methodology for the band gap tuning of perovskite crystals, enabling the fabrication of a heterogeneous or gradient band gap structure with unique optical and electronic properties.

The third example involves the use of supramolecular gels derived from low-molecular-mass compounds that are formed through the self-assembly of molecules with multiple noncovalent weak interactions such as hydrogen bonding, dipole–dipole interactions, van der Waals forces, and solute–solvent interactions. The transition from solution to gel occurs at an elevated solute concentration, so optical force acts as a new perturbation for assembling gelator molecules. Supramolecular gelators with an azobenzene-based biscalix[4]arene exhibit unique assembly formation (63), which accompanies the morphological change into the assembly (**Figure 8*c***). In optical trapping at the solution surface, a supramolecular assembly is formed at the focal spot. The strong optical force results in a specific molecular association structure, and the resultant stable assembly spontaneously increases in size. Upon switching off the laser, needle-like structures are generated at the assembly surface, transforming it into a structure with a stable sea urchin–like morphology. The molecular association pinned at the focal spot undergoes relaxation, and the constituent molecules reorient due to their intrinsic weak intermolecular interactions, producing a morphological change in the assembly. This shows that laser trapping is a new and promising

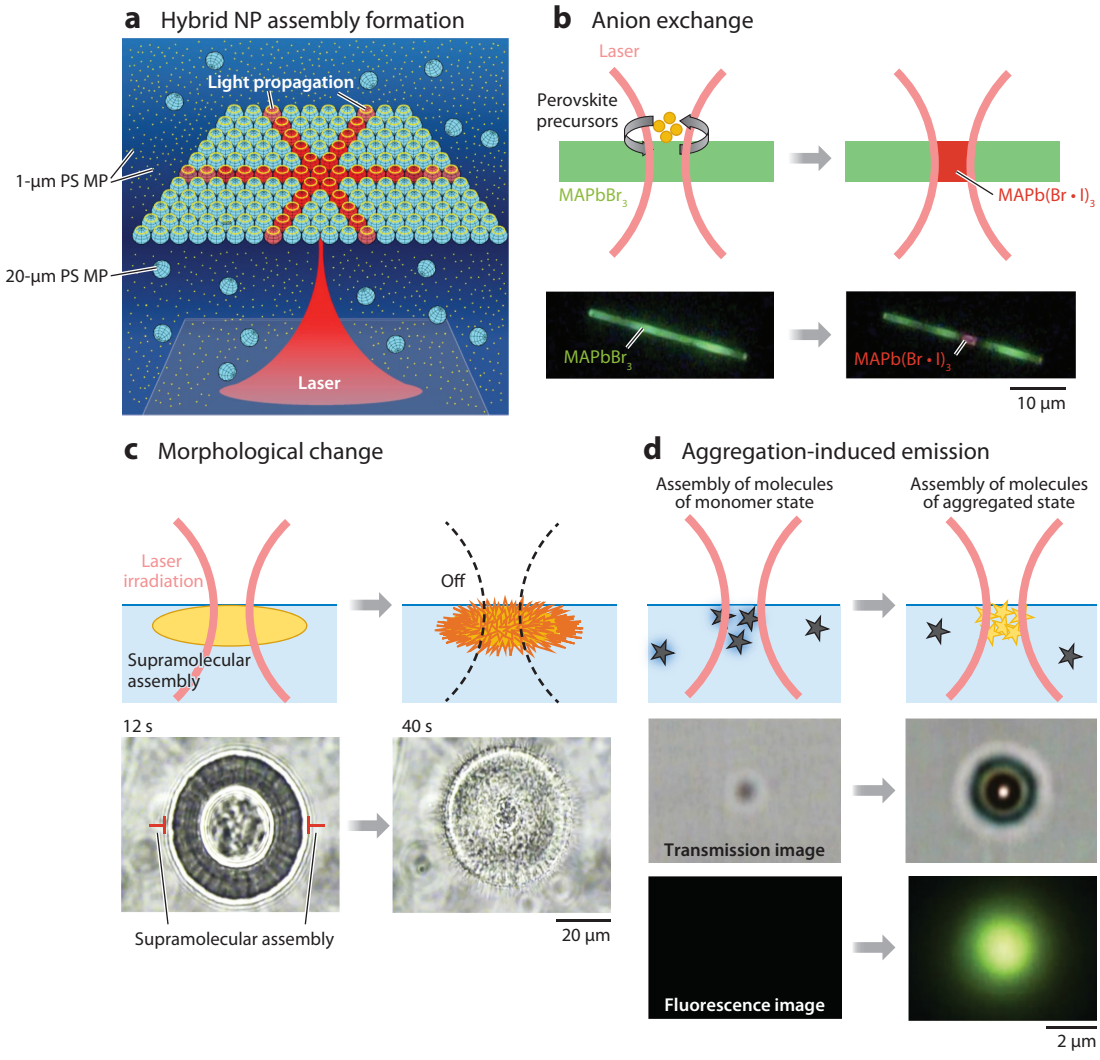

Figure 8

(*a*) Schematic illustration of a huge submillimeter-scale arrangement of a necklace-like hybrid colloidal assembly of 1-μm and 20-μm polystyrene (PS) microparticles (MPs) by optical trapping. (*b*) Illustration and micrographs of a site-specific halide exchange reaction by optical trapping perovskite [MA(methylammonium)$PbBr_3$]. Panel *b* adapted with permission from Reference 133; copyright 2020 American Chemical Society. (*c*) Illustration and micrographs of the formation of a supramolecular assembly accompanying morphological change after switching off the trapping laser. Panel *c* adapted with permission from Reference 63; copyright 2017 American Chemical Society. (*d*) Illustration and micrographs of an aggregation-induced emission during laser trapping. Panel *d* adapted with permission from Reference 134; copyright 2020 John Wiley & Sons.

approach for preparing a single spherical assembly of supramolecules, analyzing its assembly dynamics, and fabricating microstructures from single assemblies.

The fourth application involves an aggregation-induced emission enhancement (AIEE) of a tetraphenylethylene (TPE) derivative known as AIEE-active dye. Upon laser irradiation, TPE monomers undergo conformational transformation, and photoexcitation energy is dissipated via a nonradiative pathway. As a result, TPE monomers exhibit weak, almost negligible, emission. When

the monomers are densely aggregated and their conformational transformation is restricted, their fluorescence is greatly enhanced. This emission behavior can be used to investigate the dynamics of molecular assembly under optical trapping conditions. Upon the trapping of TPE at the solution surface, a small molecular assembly is formed at the focal spot after a few minutes (134). The small assembly has a weak, almost negligible, fluorescence. This shows that the TPE molecules constituting the small assembly continue the conformational transformation that accompanies the dissipation of the photoexcited energy. With further irradiation, the assembly continuously increases in size and suddenly strong fluorescence is generated, as shown in **Figure 8*d***. This fluorescence enhancement indicates that the assembly has changed into a densely packed aggregate in which the intrinsic repulsive force of the protonated TPE is overcome by the strong optical force. In laser trapping at an interface, local TPE concentration is efficiently increased, and intrinsic attractive and repulsive interactions are modified by the strong optical force, resulting in the formation of unique molecular assemblies.

8. CONCLUDING REMARKS

The optical trapping dynamics and mechanisms of molecules, polymers, and NPs at solution surfaces are completely different from those of conventional ones inside the solution, and their assembly sizes reach a few tens of micrometers larger than the focus. Optically evolving molecular crystals, PS NP assemblies, and Au NP swarms at surfaces are described and discussed, in which the gathering, trapping, arrangement, ejection, repulsion, and swarming processes are all driven by optical force. This review indicates that a new chemistry field is being paved by optical trapping at solution surfaces and that new applications are possible.

The development of optically evolved assembling is being advanced by designing new experiments. One is plasmonic trapping, which is currently receiving a large amount of attention because of the recent enhancement of optical force itself (135–141). In such experiments, metal nanostructures and semiconductor needles are fabricated on their substrates. The surface and interface leading to scattering and propagation of the trapping laser may also be involved in plasmonic trapping. For example, morphology control and enantioselectivity in molecular crystallization are being demonstrated by plasmonic trapping at the solution surface.

Another way to enhance optical force is to use the optical resonance effect in which the trapping laser wavelength matches the electronic transitions of molecules and NPs in the trapping target (142–144). In this method, optical stiffness and trapping time are used as measures of enhancement. Usually this technique is carried out in solution, but its extension to the solution/glass interface should enable us to study the optical resonance effect of not only the gradient force but also the scattering and absorption forces. This is due to the NPs being immobilized at the interface by being pushed by scattering and absorption forces.

The introduction of various microscopic techniques should allow the optically evolving assembly and swarming of molecules and NPs to be studied more widely and in greater detail. Single-molecule fluorescence microscopy and super-resolution analysis should enable us to extend dynamics and mechanism studies to nanometer-scale resolution (9, 10). Multiplane microscopy will provide 3D information on optical trapping dynamics (145), while dynamic differential microscopy will be useful to elucidate 2D assembling dynamics, as in **Figure 7** (146).

Further, pulsed lasers are useful to explore new optically evolved assembling and swarming phenomena. We have extended femtosecond studies on the optical trapping dynamics of PS NPs in solution, found trapping and ejection behavior, and proposed a mechanism based on the transient assembly formation of PS NPs in the optical potential (147–150). The assembly becomes large, the scattering force overcomes the gradient force, and then the assembly is ejected from the

optical potential. Such femtosecond optical trapping can be extended to solution surfaces, which will enable us to explore new optical force–induced molecular phenomena. Thus, the study of the optically evolved assembling of molecules and NPs is fundamentally important and provides promising materials applications that will be more fully developed by new types of microscopy and related tools and by theoretical analysis. We hope that our viewpoint, illustrated in **Figure 1**, will be more widely developed and more deeply elucidated and that a new research field of optical force–induced chemistry will open up.

DISCLOSURE STATEMENT

The authors are not aware of any affiliations, memberships, funding, or financial holding that might be perceived as affecting the objectivity of this review.

ACKNOWLEDGMENTS

This review is dedicated to the late Arthur Ashkin for his pioneering work on optical trapping and his kind understanding of our extensive use of optical trapping techniques in the field of microchemistry. The authors would like to express their sincere thanks to Teruki Sugiyama of National Chiao Tung University in Taiwan and Tetsuhiro Kudo of Toyota Technological Institute in Japan for their long-term collaborations and invaluable discussions. Thanks are also due to Abdullah Kamit for his kind help with preparation of the manuscript. This work is supported by the Ministry of Science and Technology, Taiwan (grant MOST 109-2634-F-009-028) and the Center for Emergent Functional Matter Science of the National Chiao Tung University from The Featured Areas Research Center Program within the framework of the Higher Education Sprout Project by the Ministry of Education in Taiwan. Thanks are also due for funding from the Ministry of Science and Technology (MOST) of Taiwan (grant MOST 109-2113-M-009-022 to H.M.), to the Japan Society for the Promotion of Science (grant JSPS-KAKENHI JP20K05242 to K.Y.), and to the Japan Science and Technology Agency (grant JST-CREST JPMJCR1903 to K.Y.).

LITERATURE CITED

1. Maiman TH. 1960. Stimulated optical radiation in ruby. *Nature* 187:493–94
2. Moore CB. 1971. Lasers in chemistry. *Annu. Rev. Phys. Chem.* 22:387–428
3. Porter G, Topp MR. 1970. Nanosecond flash photolysis. *Proc. R. Soc. A Math. Phys. Eng. Sci.* 315:163–84
4. Novak JR, Windsor MW. 1967. Laser photolysis and spectroscopy in the nanosecond time range: excited singlet state absorption in coronene. *J. Chem. Phys.* 47:3075–76
5. Eisert WG, Degenkolb EO, Noe LJ, Rentzepis PM. 1979. Kinetics of carboxymyoglobin and oxymyoglobin studied by picosecond spectroscopy. *Biophys. J.* 25:455–64
6. Potter ED, Herek JL, Pedersen S, Liu Q, Zewail AH. 1992. Femtosecond laser control of a chemical reaction. *Nature* 355:66–68
7. Wang XF, Herman B, eds. 1996. *Fluorescence Imaging Spectroscopy and Microscopy*. Vol. 137. New York: John Wiley & Sons
8. Rigler R, Orrit M, Basché T, eds. 2001. *Single Molecule Spectroscopy: Nobel Conference Lectures*. Springer Ser. Chem. Phys. Vol. 67. Berlin/New York: Springer
9. Sauer M, Hofkens J, Enderlein J, eds. 2011. *Handbook of Fluorescence Spectroscopy and Imaging: From Ensemble to Single Molecules*. Hoboken, NJ: John Wiley & Sons
10. Masters BR. 2020. *Superresolution Optical Microscopy: The Quest for Enhanced Resolution and Contrast*. Springer Ser. Opt. Sci. Vol. 227. Cham, Switz.: Springer
11. Moerner WE. 2002. A dozen years of single-molecule spectroscopy in physics, chemistry, and biophysics. *J. Phys. Chem. B* 106:910–27

12. Ashkin A, Dziedzic JM, Bjorkholm JE, Chu S. 1986. Observation of a single-beam gradient force optical trap for dielectric particles. *Opt. Lett.* 11:288–90
13. Lebedev PN. 1901. Experimental examination of light pressure. *Ann. Phys.* 6:433
14. Grier DG. 2003. A revolution in optical manipulation. *Nature* 424:810–16
15. Neuman KC, Block SM. 2004. Optical trapping. *Rev. Sci. Instrum.* 75:2787–809
16. Moffitt JR, Chemla YR, Smith SB, Bustamante C. 2008. Recent advances in optical tweezers. *Annu. Rev. Biochem.* 77:205–28
17. Dholakia K, Reece P, Gu M. 2008. Optical micromanipulation. *Chem. Soc. Rev.* 37:42–45
18. Padgett M, Bowman R. 2011. Tweezers with a twist. *Nat. Photon.* 5:343–48
19. Juan ML, Righini M, Quidant R. 2011. Plasmon nano-optical tweezers. *Nat. Photon.* 5:349–56
20. Sugiyama T, Yuyama K, Masuhara H. 2012. Laser trapping chemistry: from polymer assembly to amino acid crystallization. *Acc. Chem. Res.* 45:1946–54
21. Maragò OM, Jones PH, Gucciardi PG, Volpe G, Ferrari AC. 2013. Optical trapping and manipulation of nanostructures. *Nat. Nanotechnol.* 8:807–19
22. Woerdemann M, Alpmann C, Esseling M, Denz C. 2013. Advanced optical trapping by complex beam shaping. *Laser Photon. Rev.* 7:839–54
23. Lehmuskero A, Johansson P, Rubinsztein-Dunlop H, Tong L, Käll M. 2015. Laser trapping of colloidal metal nanoparticles. *ACS Nano* 9:3453–69
24. Daly M, Sergides M, Chormaic SN. 2015. Optical trapping and manipulation of micrometer and submicrometer particles. *Laser Photon. Rev.* 3:309–29
25. Spesyvtseva SES, Dholakia K. 2016. Trapping in a material world. *ACS Photon*. 3:719–36
26. Rodríguez-Sevilla P, Labrador-Páez L, Jaque D, Haro-González P. 2017. Optical trapping for biosensing: materials and applications. *J. Mater. Chem. B* 5:9085–101
27. Gao D, Ding W, Nieto-Vesperinas M, Ding X, Rahman M, et al. 2017. Optical manipulation from the microscale to the nanoscale: fundamentals, advances and prospects. *Light Sci. Appl.* 6:e17039
28. Bradshaw DS, Andrews DL. 2017. Manipulating particles with light: radiation and gradient forces. *Eur. J. Phys.* 38:034008
29. Bradac C. 2018. Nanoscale optical trapping: a review. *Adv. Opt. Mater.* 6:1800005
30. Zemánek P, Volpe G, Jonáš A, Brzobohatý O. 2019. Perspective on light-induced transport of particles: from optical forces to phoretic motion. *Adv. Opt. Photon.* 11:577–678
31. Bustamante C, Alexander L, Maciuba K, Kaiser CM. 2020. Single-molecule studies of protein folding with optical tweezers. *Annu. Rev. Biochem.* 89:443–70
32. Ashkin A. 1970. Acceleration and trapping of particles by radiation pressure. *Phys. Rev. Lett.* 24:156–59
33. Ashkin A. 1980. Application of laser radiation pressure. *Science* 210:1081–88
34. Ashkin A, Dziedzic JM. 1987. Optical trapping and manipulation of viruses and bacteria. *Science* 235:1517–20
35. Ashkin A, Dziedzic JM, Yamane T. 1987. Optical trapping and manipulation of single cells using infrared laser beams. *Nature* 330:769–71
36. Smith SB, Cui Y, Bustamante C. 1996. Overstretching B-DNA: the elastic response of individual double-stranded and single-stranded DNA molecules. *Science* 271:795–99
37. Wang MD, Yin H, Landick R, Gelles J, Block SM. 1997. Stretching DNA with optical tweezers. *Biophys. J.* 72:1335–46
38. Sasaki K, Koshioka M, Misawa H, Kitamura N, Masuhara H. 1991. Laser-scanning micromanipulation and spatial patterning of fine particles. *Jpn. J. Appl. Phys.* 30:L907
39. Sasaki K, Koshioka M, Misawa H, Kitamura N, Masuhara H. 1992. Optical trapping of a metal particle and a water droplet by a scanning laser beam. *Appl. Phys. Lett.* 60:807–9
40. Kim H-B, Hayashi M, Nakatani K, Kitamura N, Sasaki K, et al. 1996. In situ measurements of ion-exchange processes in single polymer particles: laser trapping microspectroscopy and confocal fluorescence microspectroscopy. *Anal. Chem.* 68:409–14
41. Tamai N, Asahi T, Masuhara H. 1993. Femtosecond transient absorption microspectrophotometer combined with optical trapping technique. *Rev. Sci. Instrum.* 64:2496–503

42. Nakatani K, Uchida T, Funakura S, Sekiguchi A, Misawa H, et al. 1993. Control of a dye formation reaction in a single micrometer-sized oil-droplet by laser trapping and microelectrochemical methods. *Chem. Lett.* 22:717–20
43. Misawa H, Koshioka M, Sasaki K, Kitamura N, Masuhara H. 1991. Three-dimensional optical trapping and laser ablation of a single polymer latex particle in water. *J. Appl. Phys.* 70:3829–36
44. Ito S, Tanaka Y, Yoshikawa H, Ishibashi Y, Miyasaka H, Masuhara H. 2011. Confinement of photopolymerization and solidification with radiation pressure. *J. Am. Chem. Soc.* 133:14472–75
45. Masuhara H, De Schryver FC, Kitamura N, Tamai N, eds. 1994. *Microchemistry: Spectroscopy and Chemistry in Small Domains*. North-Holland Delta Ser. Amsterdam: Elsevier Sci.
46. Masuhara H, De Schryver FC, eds. 1999. *Organic Mesoscopic Chemistry*. Malden, MA: Blackwell Sci.
47. Ashkin A. 1997. Optical trapping and manipulation of neutral particles using lasers. *PNAS* 94:4853–60
48. Ashkin A. 2000. History of optical trapping and manipulation of small-neutral particle, atoms, and molecules. *IEEE J. Sel. Top. Quantum Electron.* 6:841–56
49. Lett PD, Julienne PS, Phillips WD. 1995. Photoassociative spectroscopy of laser-cooled atoms. *Annu. Rev. Phys. Chem.* 46:423–52
50. Tsuboi Y, Shoji T, Kitamura N. 2007. Crystallization of lysozyme based on molecular assembling by photon pressure. *Jpn. J. Appl. Phys.* 46:L1234
51. Tsuboi Y, Shoji T, Nishino M, Masuda S, Ishimori K, Kitamura N. 2009. Optical manipulation of proteins in aqueous solution. *Appl. Surf. Sci.* 255:9906–8
52. Tsuboi Y, Shoji T, Kitamura N. 2010. Optical trapping of amino acids in aqueous solutions. *J. Phys. Chem. C* 114:5589–93
53. Shoji T, Kitamura N, Tsuboi Y. 2013. Resonant excitation effect on optical trapping of myoglobin: the important role of a heme cofactor. *J. Phys. Chem. C* 117:10691–97
54. Tanaka Y, Yoshikawa H, Masuhara H. 2006. Two-photon fluorescence spectroscopy of individually trapped pseudoisocyanine J-aggregates in aqueous solution. *J. Phys. Chem. B* 110:17906–11
55. Mototsuji A, Shoji T, Wakisaka Y, Murakoshi K, Yao H, Tsuboi Y. 2017. Plasmonic optical trapping of nanometer-sized J-/H- dye aggregates as explored by fluorescence microspectroscopy. *Opt. Express* 25:13617–25
56. Hofken J, Hotta J, Sasaki K, Masuhara H, Iwai K. 1997. Molecular assembling by the radiation pressure of a focused laser beam: poly(*N*-isopropylacrylamide) in aqueous solution. *Langmuir* 13:414–19
57. Hofkens J, Hotta J, Sasaki K, Masuhara H, Taniguchi T, Miyashita T. 1997. Molecular association by the radiation pressure of a focused laser beam: fluorescence characterization of pyrene-labeled PNIPAM. *J. Am. Chem. Soc.* 119:2741–42
58. Borowicz P, Hotta J, Sasaki K, Masuhara H. 1998. Chemical and optical mechanism of microparticle formation of poly(*N*-vinylcarbazole) in *N*,*N*-dimethylformamide by photon pressure of a focused near-infrared laser beam. *J. Phys. Chem. B* 102:1896–901
59. Smith TA, Hotta J, Sasaki K, Masuhara H, Itoh Y. 1999. Photon pressure-induced association of nanometer-sized polymer chains in solution. *J. Phys. Chem. B* 103:1660–63
60. Masuo S, Yoshikawa H, Nothofer HG, Grimsdale AC, Scherf U, et al. 2005. Assembling and orientation of polyfluorenes in solution controlled by a focused near-infrared laser beam. *J. Phys. Chem. B* 109:6917–21
61. Singer W, Nieminen TA, Heckenberg NR, Rubinsztein-Dunlop H. 2007. Collecting single molecules with conventional optical tweezers. *Phys. Rev. E* 75:011916
62. Gould OEC, Qiu H, Lunn DJ, Rowden J, Harniman RL, et al. 2015. Transformation and patterning of supermicelles using dynamic holographic assembly. *Nat. Commun.* 6:10009
63. Yuyama K, Marcelis L, Su PM, Chung WS, Masuhara H. 2017. Photocontrolled supramolecular assembling of azobenzene-based biscalix[4]arenes upon starting and stopping laser trapping. *Langmuir* 33:755–63
64. Gould OEC, Box SJ, Boott CE, Ward AD, Winnik MA, et al. 2019. Manipulation and deposition of complex, functional block copolymer nanostructures using optical tweezers. *ACS Nano* 13:3858–66
65. Katsura S, Hirano K, Matsuzawa Y, Mizuno A, Yoshikawa K. 1998. Direct laser trapping of single DNA molecules in the globular state. *Nucleic Acids Res.* 26:4943–45

66. Tan S, Lopez HA, Cai CW, Zhang Y. 2004. Optical trapping of single-walled carbon nanotubes. *Nano Lett*. 4:1415–19
67. Rodgers T, Shoji S, Sekkat Z, Kawata S. 2008. Selective aggregation of single-walled carbon nanotubes using the large optical field gradient of a focused laser beam. *Phys. Rev. Lett.* 101:127402
68. Hotta J, Sasaki K, Masuhara H. 1996. A single droplet formation from swelled micelles by radiation pressure of a focused infrared laser beam. *J. Am. Chem. Soc.* 118:11968–69
69. Kitamura N, Sekiguchi N, Kim HB. 1998. Optical transformation and fission of single giant vesicles in water by radiation pressure. *J. Am. Chem. Soc.* 120:1942–43
70. Murshid N, Yuyama K, Wu SL, Wu KY, Masuhara H, et al. 2016. Highly-integrated, laser manipulable aqueous metal carbonyl vesicles (MCsomes) with aggregation-induced emission (AIE) and aggregation-enhanced IR absorption (AEIRA). *J. Mater. Chem.* 4:5231–40
71. Pan L, Ishikawa A, Tamai N. 2007. Detection of optical trapping of CdTe quantum dots by two-photon-induced luminescence. *Phys. Rev. B* 75:161305(R)
72. Jauffred L, Oddershede LB. 2010. Two-photon quantum dot excitation during optical trapping. *Nano Lett*. 10:1927–30
73. Chiang WY, Okuhata T, Usman A, Tamai N, Masuhara H. 2014. Efficient optical trapping of CdTe quantum dots by femtosecond laser pulses. *J. Phys. Chem. B* 118:14010–16
74. Pin C, Otsuka R, Sasaki K. 2020. Optical transport and sorting of fluorescent nanodiamonds inside a tapered glass capillary: optical sorting of nanomaterials at the femtonewton scale. *ACS Appl. Nano Mater.* 3:4127–34
75. Pauzauskie PJ, Radenovic A, Trepagnier E, Shroff H, Yang P, Liphardt J. 2006. Optical trapping and integration of semiconductor nanowire assemblies in water. *Nat. Mater.* 5:97–101
76. Yan Z, Jureller JE, Sweet J, Guffey MJ, Pelton M, Scherer NF. 2012. Three-dimensional optical trapping and manipulation of single silver nanowires. *Nano Lett*. 12:5155–61
77. Yan Z, Pelton M, Vigderman L, Zubarev ER, Scherer NF. 2013. Why single-beam optical tweezers trap gold nanowires in three dimensions. *ACS Nano* 7:8794–800
78. Hosokawa C, Yoshikawa H, Masuhara H. 2005. Cluster formation of nanoparticles in an optical trap studied by fluorescence correlation spectroscopy. *Phys. Rev. E* 72:021408
79. Hosokawa C, Yoshikawa H, Masuhara H. 2004. Optical assembling dynamics of individual polymer nanospheres investigated by single-particle fluorescence detection. *Phys. Rev. E* 70:061410
80. Ito S, Yoshikawa H, Masuhara H. 2002. Laser manipulation and fixation of single gold nanoparticles in solution at room temperature. *Appl. Phys. Lett.* 80:482–84
81. Tanaka Y, Yoshikawa H, Itoh T, Ishikawa M. 2009. Laser-induced self-assembly of silver nanoparticles via plasmonic interactions. *Opt. Express* 17:18760–67
82. Jiang Y, Narushima T, Okamoto H. 2010. Nonlinear optical effects in trapping nanoparticles with femtosecond pulses. *Nat. Phys.* 6:1005–9
83. Urban AS, Lutich AA, Stefani FD, Feldmann J. 2010. Laser printing single gold nanoparticles. *Nano Lett.* 10:4794–98
84. Ohlinger A, Nedev S, Lutich AA, Feldmann J. 2011. Optothermal escape of plasmonically coupled silver nanoparticles from a three-dimensional optical trap. *Nano Lett*. 4:1770–74
85. Kyrsting A, Bendix PM, Oddershede LB. 2013. Mapping 3D focal intensity exposes the stable trapping positions of single nanoparticles. *Nano Lett*. 13:31–35
86. Harada Y, Asakura T. 1996. Radiation forces on a dielectric sphere in the Rayleigh scattering regime. *Opt. Commun.* 124:529–41
87. Ito S, Sugiyama T, Toitani N, Katayama G, Miyasaka H. 2007. Application of fluorescence correlation spectroscopy to the measurement of local temperature in solutions under optical trapping condition. *J. Phys. Chem. B* 111:2365–71
88. Chiu DT, Zare R. 1996. Biased diffusion, optical trapping, and manipulation of single molecules in solution. *J. Am. Chem. Soc.* 118:6512–13
89. Osborne MA, Balasubramanian S, Furey WS, Klenerman D. 1998. Optically biased diffusion of single molecules studied by confocal fluorescence microscopy. *J. Phys. Chem. B* 102:3160–67
90. Chirico G, Fumagalli C, Baldini G. 2002. Trapped Brownian motion in single- and two-photon excitation fluorescence correlation experiments. *J. Phys. Chem. B* 106:2508–19

91. Nabetani Y, Yoshikawa H, Grimsdale AC, Müllen K, Masuhara H. 2007. Effects of optical trapping and liquid surface deformation on the laser microdeposition of a polymer assembly in solution. *Langmuir* 23:6725–29
92. Louchev OA, Juodkazis S, Murazawa N, Wada S, Misawa H. 2008. Coupled laser molecular trapping, cluster assembly, and deposition fed by laser-induced Marangoni convection. *Opt. Express* 16:5673–80
93. Bartkiewicz S, Miniewicz A. 2015. Whirl-enhanced continuous wave laser trapping of particles. *Phys. Chem. Chem. Phys.* 17:1077–83
94. Yuyama K, Sugiyama T, Masuhara H. 2010. Millimeter-scale dense liquid droplet formation and crystallization in glycine solution induced by photon pressure. *J. Phys. Chem. Lett.* 1:1321–25
95. Yuyama K, Rungsimanon T, Sugiyama T, Masuhara H. 2012. Formation, dissolution, and transfer dynamics of a millimeter-scale thin liquid droplet in glycine solution by laser trapping. *J. Phys. Chem. C* 116:6809–16
96. Sugiyama T, Adachi T, Masuhara H. 2007. Crystallization of glycine by photon pressure of a focused CW laser beam. *Chem. Lett.* 36:1480–81
97. Rungsimanon T, Yuyama K, Sugiyama T, Masuhara H, Tohnai N, Miyata M. 2010. Control of crystal polymorph of glycine by photon pressure of a focused continuous wave near-infrared laser beam. *J. Phys. Chem. Lett.* 1:599–603
98. Rungsimanon T, Yuyama K, Sugiyama T, Masuhara H. 2010. Crystallization in unsaturated glycine/D_2O solution achieved by irradiating a focused continuous wave near infrared laser. *Cryst. Growth Des.* 10:4686–88
99. Yuyama K, Rungsimanon T, Sugiyama T, Masuhara H. 2012. Selective fabrication of α- and γ-polymorphs of glycine by intense polarized continuous wave laser beams. *Cryst. Growth Des.* 12:2427–34
100. Yuyama K, Ishiguro K, Sugiyama T, Masuhara H. 2012. Laser trapping dynamics of L-alanine depending on the laser polarization. In *Proceedings SPIE 8458: Optical Trapping and Optical Micromanipulation IX*, ed. K Dholakia, GC Spalding, pp. 84582D-1–7. Bellingham, WA: SPIE
101. Yuyama K, Sugiyama T, Masuhara H. 2013. Laser trapping and crystallization dynamics of L-phenylalanine at solution surface. *J. Phys. Chem. Lett.* 4:2436–40
102. Yuyama K, Wu CS, Sugiyama T, Masuhara H. 2014. Laser trapping-induced crystallization of L-phenylalanine through its high-concentration domain formation. *Photochem. Photobiol. Sci.* 13:254–60
103. Yuyama K, George J, Thomas KG, Sugiyama T, Masuhara H. 2016. Two-dimensional growth rate control of L-phenylalanine crystal by laser trapping in unsaturated aqueous solution. *Cryst. Growth Des.* 16:953–60
104. Yuyama K, Chiu DS, Liu YE, Sugiyama T, Masuhara H. 2018. Crystal growth and dissolution dynamics of L-phenylalanine controlled by solution surface laser trapping. *Cryst. Growth Des.* 18:7079–87
105. Chen JJ-K, Yuyama K, Sugiyama T, Masuhara H. 2019. In situ reflection imaging and microspectroscopic study on three-dimensional crystal growth of L-phenylalanine under laser trapping. *Appl. Phys. Express* 12:112008
106. Cheng AC, Masuhara H, Sugiyama T. 2020. Evolving crystal morphology of potassium chloride controlled by optical trapping. *J. Phys. Chem. C* 124:6913–21
107. Niinomi H, Sugiyama T, Miyamoto K, Omatsu T. 2018. "Freezing" of $NaClO_3$ metastable crystalline state by optical trapping in unsaturated microdroplet. *Cryst. Growth Des.* 18:734–41
108. Yuyama K, Islam MJ, Takahashi K, Nakamura T, Biju V. 2018. Crystallization of methylammonium lead halide perovskites by optical trapping. *Angew. Chem. Int. Ed.* 57:13424–28
109. Islam MJ, Yuyama K, Takahashi K, Nakamura T, Konishi K, Biju V. 2019. Mixed-halide perovskite synthesis by chemical reaction and crystal nucleation under an optical potential. *NPG Asia Mater.* 11:31
110. Wang SF, Kudo T, Yuyama K, Sugiyama T, Masuhara H. 2016. Optically evolved assembly formation in laser trapping of polystyrene nanoparticles at solution surface. *Langmuir* 32:12488–96
111. Lu JS, Kudo T, Louis B, Bresolí-Obach R, Scheblykin IG, et al. 2020. Optical force-induced dynamics of assembling, rearrangement, and three-dimensional pistol-like ejection of microparticles at the solution surface. *J. Phys. Chem. C* 124:27107–17
112. Nam HJ, Jung D-Y, Yi G-R, Choi H. 2006. Close-packed hemispherical microlens array from two-dimensional ordered polymeric microspheres. *Langmuir* 22:7358–63

113. Shoji T, Shibata M, Kitamura N, Nagasawa F, Takase M. et al. 2013. Reversible photoinduced formation and manipulation of a two-dimensional closely packed assembly of polystyrene nanospheres on a metallic nanostructure. *J. Phys. Chem. C* 117:2500–6
114. Wang SF, Yuyama K, Sugiyama T, Masuhara H. 2016. Reflection microspectroscopic study of laser trapping assembling of polystyrene nanoparticles at air/solution interface. *J. Phys. Chem. C* 120:15578–85
115. Kudo T, Wang S-F, Yuyama K, Masuhara H. 2016. Optical trapping-formed colloidal assembly with horns extended to the outside of a focus through light propagation. *Nano Lett*. 16:3058–62
116. Kudo T, Yang S-J, Masuhara H. 2018. A single large assembly with dynamically fluctuating swarms of gold nanoparticles formed by trapping laser. *Nano Lett*. 18:5846–53
117. Huang C-H, Kudo T, Bresolí-Obach R, Hofkens J, Sugiyama T, Masuhara H. 2020. Surface plasmon resonance effect on laser trapping and swarming of gold nanoparticles at interface. *Opt. Express* 28:27727–35
118. Aibara I, Huang C-H, Kudo T, Bresolí-Obach R, Hofkens J, et al. 2020. Dynamic coupling of optically evolved assembling and swarming of gold nanoparticles with photothermal local phase separation of polymer solution. *J. Phys. Chem. C* 124:16604–15
119. Kuppe C, Rusimova KR, Ohnoutek L, Slavov D, Valev VK. 2020. "Hot" in plasmonics: temperature-related concepts and applications of metal nanostructures. *Adv. Opt. Mater.* 8:1901166
120. Setoura K, Ito S, Miyasaka H. 2017. Stationary bubble formation and Marangoni convection induced by CW laser heating of a single gold nanoparticle. *Nanoscale* 9:719–30
121. Heskins M, Guillet JE. 1968. Solution properties of poly(N-isopropylacrylamide). *J. Macromol. Sci. A* 2:1441–55
122. Hashimoto C, Ushiki H. 2006. Graphical analysis for gel morphology. III. Gel size and temperature effects on the volume phase transition of gels. *J. Chem. Phys.* 124:044903
123. Aibara I, Mukai S, Hashimoto S. 2016. Plasmonic-heating-induced nanoscale phase separation of free poly(*N*-isopropylacrylamide) molecules. *J. Phys. Chem. C* 120:17745–52
124. Aibara I, Chikazawa JI, Uwada T, Hashimoto S. 2017. Localized phase separation of thermoresponsive polymers induced by plasmonic heating. *J. Phys. Chem. C* 121:22496–507
125. Braun D, Libchaber A. 2002. Trapping of DNA by thermophoretic depletion and convection. *Phys. Rev. Lett.* 89:188103
126. Young JB. 2011. Thermophoresis of a spherical particle: reassessment, clarification, and new analysis. *Aerosol Sci. Technol.* 45:927–48
127. Leng J, Guo Z, Zhang H, Chang T, Guo X, Gao H. 2016. Negative thermophoresis in concentric carbon nanotube nanodevices. *Nano Lett*. 16:6396–402
128. Wu CL, Wang SF, Kudo T, Yuyama K, Sugiyama T, Masuhara H. 2020. Anomalously large assembly formation of polystyrene nanoparticles by optical trapping at solution surface. *Langmuir* 36:14234–42
129. Taschin A, Bartolini P, Eramo R, Righini R, Torre R. 2014. Optical Kerr effect of liquid and supercooled water: the experimental and data analysis perspective. *J. Chem. Phys.* 141:084507
130. Garetz BA, Aber JE, Goddard NL, Young RG, Myerson AS. 1996. Nonphotochemical, polarization-dependent, laser-induced nucleation in supersaturated aqueous urea solution. *Phys. Rev. Lett.* 77:3475–76
131. Maloney RC, Hall CK. 2020. Clustering and phase separation in mixtures of dipolar and active particles in an external field. *Langmuir* 36:6378–87
132. Lu J-S, Wang H-Y, Kudo T, Masuhara M. 2020. A large submillimeter assembly of microparticles with necklace-like patterns formed by laser trapping at solution surface. *J. Phys. Chem. Lett.* 11:6057–62
133. Islam MJ, Shahjahan M, Yuyama K, Biju V. 2020. Remote tuning of bandgap and emission of lead perovskites by spatially controlled halide exchange reactions. *ACS Mater. Lett.* 2:403–8
134. Wang S-F, Lin J-R, Ishiwari F, Fukushima T, Masuhara H, Sugiyama T. 2020. Spatiotemporal dynamics of aggregation-induced emission enhancement controlled by optical manipulation. *Angew. Chem. Int. Ed.* 59:7063–68
135. Kawata S, Masuhara H, eds. 2006. *Nanoplasmonics: from Fundamentals to Applications*. Amsterdam: Elsevier
136. Tsai W-Y, Huang J-S, Huang C-B. 2014. Selective trapping or rotation of isotropic dielectric microparticles by optical near field in a plasmonic Archimedes spiral. *Nano Lett*. 14:547–52

137. Shoji T, Saitoh J, Kitamura N, Nagasawa F, Murakoshi K, et al. 2013. Permanent fixing or reversible trapping and release of DNA micropatterns on a gold nanostructure using continuous-wave or femtosecond-pulsed near-infrared laser light. *J. Am. Chem. Soc.* 135:6643–48
138. Kotsifaki DG, Chormaic SN. 2019. Plasmonic optical tweezers based on nanostructures: fundamentals, advances and prospects. *Nanophoton* 8:1227–45
139. Shoji T, Itoh K, Saitoh J, Kitamura N, Yoshii T, et al. 2020. Plasmonic manipulation of DNA using a combination of optical and thermophoretic forces: separation of different-sized DNA from mixture solution. *Sci. Rep.* 10:3349
140. Shoji T, Mototsuji A, Balčytis A, Linklater D, Juodkazis S, Tsuboi Y. 2017. Optical tweezing and binding at high irradiation powers on black-Si. *Sci. Rep.* 7:12298
141. Hanasaki I, Shoji T, Tsuboi Y. 2019. Regular assembly of polymer nanoparticles by optical trapping enhanced with a random array of Si needles for reconfigurable photonic crystals in liquid. *ACS Appl. Nano Mater.* 2:7637–43
142. Hosokawa C, Yoshikawa H, Masuhara H. 2006. Enhancement of biased diffusion of dye-doped nanoparticles by simultaneous irradiation with resonance and nonresonance laser beams. *Jpn. J. Appl. Phys.* 45:L453
143. Kudo T, Ishihara H. 2012. Proposed nonlinear resonance laser technique for manipulating nanoparticles. *Phys. Rev. Lett.* 109:087402
144. Kudo T, Ishihara H, Masuhara H. 2017. Resonance optical trapping of individual dye-doped polystyrene particles with blue- and red-detuned lasers. *Opt. Express* 25:4655–64
145. Louis B, Camacho R, Bresolí-Obach R, Abakumov S, Vandaele J, et al. 2020. Fast-tracking of single emitters in large volumes with nanometer precision. *Opt. Express* 28:28656–71
146. Hanasaki I, Okano K, Yoshikawa HY, Sugiyama T. 2019. Spatiotemporal dynamics of laser-induced molecular crystal precursors visualized by particle image diffusometry. *J. Phys. Chem. Lett.* 10:7452–57
147. Usman A, Chiang W-Y, Masuhara H. 2012. Optical trapping and polarization-controlled scattering of dielectric spherical nanoparticles by femtosecond laser pulses. *J. Photochem. Photobiol. A Chem.* 234:83–90
148. Chiang W-Y, Usman A, Masuhara H. 2013. Femtosecond pulse-width dependent trapping and directional ejection dynamics of dielectric nanoparticles. *J. Phys. Chem. C* 117:19182–88
149. Muramatsu M, Shen T-F, Chiang W-Y, Usman A, Masuhara H. 2016. Picosecond motional relaxation of nanoparticles in femtosecond laser trapping. *J. Phys. Chem. C* 120:5251–56
150. Chiang W-Y, Chen JJ-K, Usman A, Kudo T, Xia K, et al. 2019. Formation mechanism and fluorescence characterization of a transient assembly of nanoparticles generated by femtosecond laser trapping, *J. Phys. Chem. C* 123:27823–33